Energy Conversion and Management: X 24 (2024) 100806

Contents lists available at ScienceDirect

Energy Conversion and Management: X

journal homepage: www.sciencedirect.com/journal/energy-conversion-and-management-x

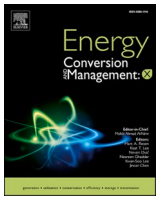

Salt hydrate based thermochemical systems cascaded with high temperature mechanical heat pumps for waste heat recovery

K. Malleswararao [a,*], Inga Bürger [a], Aldo Cosquillo Mejia [a], Seon Tae Kim [b], Marc Linder [a]

[a] Institute of Engineering Thermodynamics, German Aerospace Center (DLR), Pfaffenwaldring 38-40, Stuttgart 70569, Germany
[b] Institute of Low-Carbon Industrial Process, German Aerospace Center (DLR), Mandau-Höfe, Äußere Oybiner Straße 14/16, Zittau 02763, Germany

ARTICLE INFO

Keywords:
High temperature heat pump
Waste heat recovery
Thermochemical energy
Thermochemical heat transformer
Salt hydrates
Cascaded heat pump

ABSTRACT

The efficient use of waste heat is essential for addressing global energy needs and achieving carbon neutrality targets. High-Temperature Heat Pumps (HTHPs) play an important role in this endeavor. However, for their efficient operation, these devices need a continuous supply of heat at temperatures higher than their evaporators' temperatures. As a result, heat at temperatures below HTHP's evaporator temperature is wasted. This study aims to design and thermodynamically analyze a cascaded system where, next to the HTHP, a thermochemical system based on salt hydrates is integrated, which is able to upgrade the low-grade waste heat of the HTHP. The system incorporates a dual-reactor salt hydrate configuration in which the HTHP's waste heat is utilized in two steps: as a driving force to generate water vapour that reacts in one reactor, producing higher temperature heat, and to charge the other reactor. The present study focuses mainly on the heat recovery performance of the thermochemical heat transformer or heat pump coupled with the HTHP. The study emphasizes the need for open reactor operation and presents a procedure for screening appropriate salt hydrates. A thermodynamic analysis is presented to evaluate the merits of the optimal system. Notably, using K_2CO_3 salt hydrate, thermodynamic analysis shows promising performance, delivering heat of 62.28 kW per kg/s of air at 57.81 % efficiency at 145 °C. The cascaded system has an overall efficiency of 85.33 % at 145 °C, with an estimated heat upgrading efficiency of 49.33 %.

Introduction

Energy systems with high efficiency and heat/temperature upgrading capability are most appropriate for addressing the energy demands of the growing population while also minimizing greenhouse gas emissions and attaining carbon neutrality. For this purpose, several studies have proposed the use of High Temperature Heat Pumps (HTHPs) as one potential strategy [1–4]. HTHPs are devices that transform heat at a low-temperature to a high-temperature using external energy input. This external energy could be electricity for mechanical heat pumps or heat for Thermochemical Heat Transformers (THT) or thermochemical heat pumps. Chua et al. [1] and Sandvall et al. [2] emphasized the significance and possible applications of HTHPs. Dong et al. [3] highlighted the role of cascaded HTHPs and examined various design conditions based on energetic and economic performance. Simulation analysis of Jarre et al. [4] suggests that using heat pumps in the power and heating sectors can result in energy savings of 10–40 % when compared to standard natural gas boilers. The experimental investigations of Lee [5] also demonstrated that HTHPs can facilitate emission-free automobiles. Gaur et al. [6] provided a comprehensive review highlighting that HTHPs enhance energy efficiency and reduce fossil fuel dependence, leading to lower CO_2 emissions.

It is understood from the literature that there is no precise consensus on the term 'high temperature' in heat pump research. Some studies used it to refer to heat sink temperatures of 75 °C–90 °C [7,8], others for 110 °C [9], some for 150 °C–160 °C [10–12], and it has recently been used to refer to temperatures up to 200 °C [13,14]. In this study, HTHP refers to using a heat source below 150 °C with the heat sink above 150 °C. Kosmadakis et al. [12] performed a techno-economic analysis to investigate the feasibility of HTHPs for upgrading low temperature waste heat up to 150 °C. They reported that HTHPs are viable for temperature uplifting up to 150 °C and suggested that two-stage heat pumps are more suitable when the required temperature uplift is more than 50 °C. Wu et al. [11] conducted experimental studies on an HTHP with R178 as a working fluid and demonstrated its capability to upgrade heat from below 100 °C to 150 °C. Using an evaporator temperature of 85 °C, they could achieve a condensation temperature of 150 °C with a

* Corresponding author.
E-mail address: malleswararao.katamala@dlr.de (K. Malleswararao).

https://doi.org/10.1016/j.ecmx.2024.100806
Received 27 August 2024; Received in revised form 7 November 2024; Accepted 21 November 2024
Available online 26 November 2024

Nomenclature

c_p	Specific heat capacity (J/kg.K)
h	Enthalpy (J/kg)
$\dot{m}$	Mass flow rate (kg/s)
n	Stochiometric coefficient
p	Pressure (bar or kPa)
$\dot{Q}$	Heat transfer rate (W)
$\widetilde{R}$	Universal gas constant (J/mol.K)
T	Temperature (K or °C)
W	Compressor work (J)

Greek letters

ΔH_r^o	Enthalpy of reaction (J/mol)
ΔH_e	Latent heat of evaporation (J/kg)
ΔH_c	Latent heat of condensation (J/kg)
ΔS_r^o	Entropy of reaction (J/mol.K)
η	Efficiency (%)
ϕ	Relative humidity (1)
ω	Specific humidity (kg water vapourper kg dry air)

Subscripts

a	Ambient/dry air
c	Condenser
cv	Control volume
dh	Dehydration
E	Evaporator
g	Saturated gas
h	Hydration
i	Initial state
in	Inlet
out	Outlet
r	Reaction
R	Reactor
v	Unsaturated gas
w	Water
wv	Water vapour

Abbreviations

COP	Coefficient of performance
HTF	Heat transfer fluid
HTHP	High temperature heat pump
TCES	Thermochemical energy storage
THT	Thermochemical heat transformer

Coefficient of Performance (COP) of 1.96. Also, using an evaporator at 75 °C, they achieved a COP of 1.85 with the condenser at 140 °C. Recently, Liu et al. [15] developed a prototype of hybrid mechanical-absorption HTHP for steam production and demonstrated the production of process steam at a temperature higher than 150 °C. The study was aimed at utilizing the waste heat of flue gases as a heat source. Using a heat source in the range of 80 °C to 170 °C, the system produced steam at 154 °C and 5.3 bar pressure. The output heat of the system was estimated to be 70.15 kW, of which the waste heat share was about 81.1 % and the share of electric heating was 18.9 %. Several studies on different types of HTHP, including hybrid systems with varying temperature levels, have demonstrated its potential for temperature uplifting in a variety of thermal applications. Liu et al. [16] proposed an advanced ammonia-water hybrid heat pump that recovers heat from flue gases below 150 °C to generate steam, achieving a COP of 5.49. Mateu-Royo et al. [17] evaluated five HTHP configurations, finding that advanced designs can decrease CO_2 emissions by up to 68 % compared to natural gas boilers [18].

Even though HTHPs are energy efficient and environmentally friendly, there are two major constraints regarding their operation. One is that heat pumps are continuously operated systems that would require additional energy storage components to effectively integrate fluctuating energy streams, and the other is that they require heat supply at a temperature higher than their evaporators' temperature. As a result, heat at temperatures below the minimum temperature of an evaporator goes unutilized, and it is considered 'waste heat' for the HTHP. In general, the heat at the outlet of the evaporator of an HTHP, at a temperature lower than its operating temperature, is disposed of in the surroundings. That heat, if collected and upgraded to the required inlet temperature of the evaporator without using electricity, would further enhance the energy utilization efficiency and total energy output as well. As a result, it can be advantageous to integrate an HTHP with a continuous heat supply system that can collect heat (thermal energy) at lower temperatures, upgrade it, and deliver it at the required temperatures of the evaporator.

Collection of thermal energy can be achieved by virtue of sensible heat storage, latent heat storage, and Thermo-Chemical Energy Storage (TCES). Despite the fact that sensible and latent heat storage methods are highly researched and widely used all over the globe, their inability to raise the temperature of heat makes them unsuitable for the objective of the present study. On the other hand, TCES systems based on solid–gas reversible reactions are proven to be promising for storing thermal energy at lower temperatures and delivering it at higher temperatures [18–21]. The decomposition of a solid–gas based TCES system demands heat supply as it involves an endothermic reaction, whereas the formation reaction produces heat due to an exothermic reaction. This feature of TCES enables the storage of available heat, and delivery on demand. The most conspicuous attribute of these systems is that they are pressure-dependent reaction temperature systems, which means that the temperature of the heat of formation reaction is determined by the pressure of the supplied gas. As a result, the supply of gas at higher pressures enables the production of heat at elevated temperatures, facilitating temperature upgrading. Another major distinguishing aspect of TCES is that they can operate with low-grade heat due to their inherent reaction kinetics.

Systems utilizing metal hydrides, salt hydrates, metal hydroxides, and similar materials are categorized under TCES, and have been extensively researched for various applications, including refrigeration [22] and heat pumps [23,24]. Chen et al. [23] and Hayatina et al. [24] emphasized the salient features of TCES as energy efficient and pollution-free thermal systems. Among these, salt hydrate systems are noted for their cost-effectiveness, energy efficiency, ease of operation, and safety due to their reaction with water vapor at relatively low pressures [18,20]. Therefore, these eliminate the need for high-pressure vessels and, thus, enable easy operation. Richter et al. [19] conducted experiments on a $CaCl_2$ and water vapor-based THT in closed operation, achieving a thermal upgrade of 35 K at 130 °C. In open operation, the same team reported potential thermal upgrades of up to 65 K [20]. Michel et al. [21] also studied a $CaCl_2$ THT with a packed bed reactor, reporting over 60 K temperature uplift at a specific power of 180 W/kg. It is to be noticed that they require reactors with large heat transfer surfaces due to the poor effective thermal conductivity of salt hydrates.

Owing to the necessity of integrating a TCES system to an HTHP and the associated advantages, the present study aims to propose the design of a suitable configuration of a cascaded TCES-HTHP system for collecting waste heat from an HTHP and delivering it at temperatures higher than its evaporator temperatures, while leveraging the TCES system's heat pumping properties. The study focuses mainly on the heat

recovery performance of the TCES system coupled with the HTHP. It starts with a preliminary qualitative assessment of the operational attributes of four different configurations of a cascaded HTHP. This includes three novel configurations of a dual-reactor based TCES system integrated with an HTHP and then selects the most suitable one for further assessment. The functionality of the selected configuration is described with the help of a van't Hoff plot that depicts the pressure–temperature correlation of the TCES system. In the next step, as the right choice of salt hydrates is crucial for the efficient operation of the system, its screening procedure is discussed. Finally, a thermodynamic analysis based on performance indicators such as energy output, energy efficiency, and water vapour recoverability is carried out to evaluate the performance of the combination of the configuration and the salt hydrate material. The study presents the performance of the selected configuration at various operating temperatures.

Temperature uplift using salt hydrate based TCES

The stochiometric equation of a salt hydrate based TCES operation is presented in Eq. (1), where S denotes salt, ΔH_r^o is the change in standard enthalpy of reaction (J/mol) and n is the stochiometric coefficient of water vapour.

$$S + nH_2O \leftrightarrow S \bullet nH_2O + \Delta H_r^o \tag{1}$$

In this study, charging refers to heat collection, and discharging refers to heat release. As mentioned earlier, salt hydrate based TCES are pressure-dependent temperature systems. It is essential to know the temperatures and the corresponding equilibrium pressures of a salt hydrate during charging and discharging to understand its feasibility of operation in any thermal application. For this purpose, the van't Hoff equation [25] is adopted, which relates the pressure (p_{eq}) of water vapour in equilibrium with a salt hydrate bed to its temperature (T_r). It can be written as,

$$\ln\left(\frac{p_{eq}}{p_0}\right) = \frac{\Delta S_r^o}{\widetilde{R}} - \frac{\Delta H_r^o}{\widetilde{R} T_r} \tag{2}$$

where ΔS_r^o is the change in standard entropy of reaction (J/mol.K) during the salt and water vapour interactions. $\widetilde{R}$ is the universal gas constant (J/mol.K) and p_0 is the reference pressure (1 bar). Eq. (2) also demonstrates that the supply of water vapour at higher pressures results in higher temperatures of reaction which facilitates the temperature upgrade.

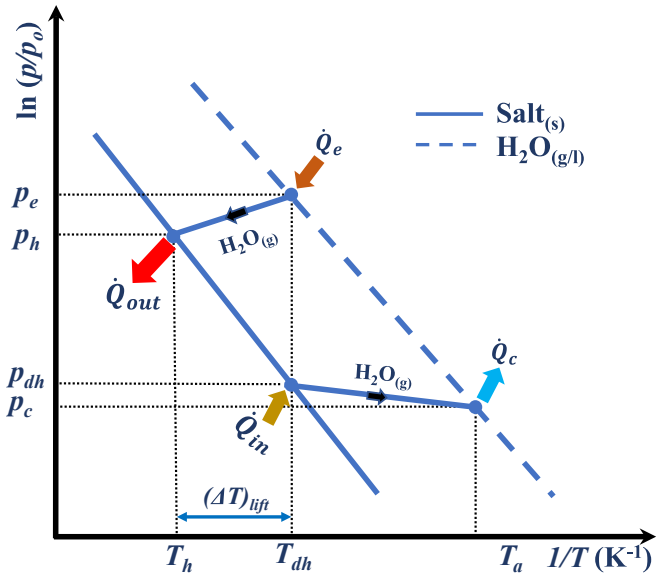

Fig. 1. Temperature upgrading using salt hydrates.

Fig. 1 depicts a simplified schematic of temperature uplift utilizing salt hydrates. During charging, low-temperature (T_{dh}) waste heat is supplied to a salt hydrate reactor, and the produced water vapour is collected using a condenser operated at ambient temperature (T_a). To discharge heat at higher temperatures (T_h), water vapour generated at higher pressures utilizing waste heat is fed into the salt hydrate reactor, resulting in higher hydration reaction temperatures. In order to realize a continuous temperature upgrade (heat pump effect), a dual-reactor system is operated in a quasi-continuous mode between the charging and discharging processes.

Configuration of a cascaded HTHP system

The primary objective of the cascaded HTHP system presented in this study is the transformation of waste heat of HTHP into useful heat that can be reintegrated in the process. For this purpose, four configurations are presented, as reported in Table 1, including a reference system of conventional cascaded HTHPs. The other three configurations consider a TCES cascaded with an HTHP through indirect and/or direct heat transfer.

In the present study, the direct heat transfer method refers to a concept, where the moist air acts as a Heat Transfer Fluid (HTF) and passes directly through the solid salt hydrate bed. The moist air serves as a reactant source (by providing water vapour for hydration), sink (by collecting water vapour for dehydration), and HTF by supplying/removing heat. TCES systems with direct heat transfer are considered open reactor systems in this study. During the charging, in an open reactor operation, hot and dry air passes directly through a porous salt hydrate bed. It provides the required heat for dehydration, collects the released water vapour, and exits the reactor in a relatively cold and humid state. During the discharging, cold and humid air passes through the anhydrous salt bed, where it provides water vapour required for the hydration and, consequently, leaves the reactor in a relatively hot and dry state by collecting the heat of hydration. This open reactor technology is expected to offer efficient heat transfer due to its lower thermal resistance and enables the maximum possible temperatures to be achieved. However, the compatibility of a salt is crucial as it is directly exposed to the air. These have been tested and demonstrated to be inexpensive, compact, well-performing with high energy storage densities, and easily manageable [26–28]. Michel et al. [27] emphasized the cost-effectiveness and adaptability of salt hydrate systems in open operation.

In contrast, in the case of indirect heat transfer, HTF flows through a heat exchanger embedded in a salt hydrate reactor, and water vapour transfers to or from the salt hydrate bed through a separate piping system. In this study, the indirect heat transfer systems are referred to as closed reactor operations. As depicted in Table 1, indirect heat transfer is proposed to be accomplished using heat pipes. Heat pipes are a well-known passive heat transfer technology that uses the phase transition of a working fluid to transfer heat without the need for any moving mechanical devices. They ensure close to isothermal and efficient heat exchange.

The present study focuses on upgrading the temperature of the waste heat of HTHPs by leveraging thermally driven heat pumps, which use waste heat (at T_0) as a driving force for their operation. Table 1 presents schematics of possible cascaded system configurations proposed in this investigation to recover waste heat from HTHPs. Because the aim of this study is to make use of waste heat sources, the systems provided in Table 1 assume the presence of a steady waste heat supply, such as industrial exhaust or process heat, which is referred to as a 'heat source' in this study.

Configuration 1 can be seen as reference as it consists of a cascaded setup featuring an HTHP, denoted as HP1, alongside a low-temperature HP, denoted as HP2. This cascaded configuration is used to compare with the other configurations of thermally driven chemical heat pumps.

Table 1
Configurations of the cascaded HTHP system and their attributes.

System configuration	Pros and Cons
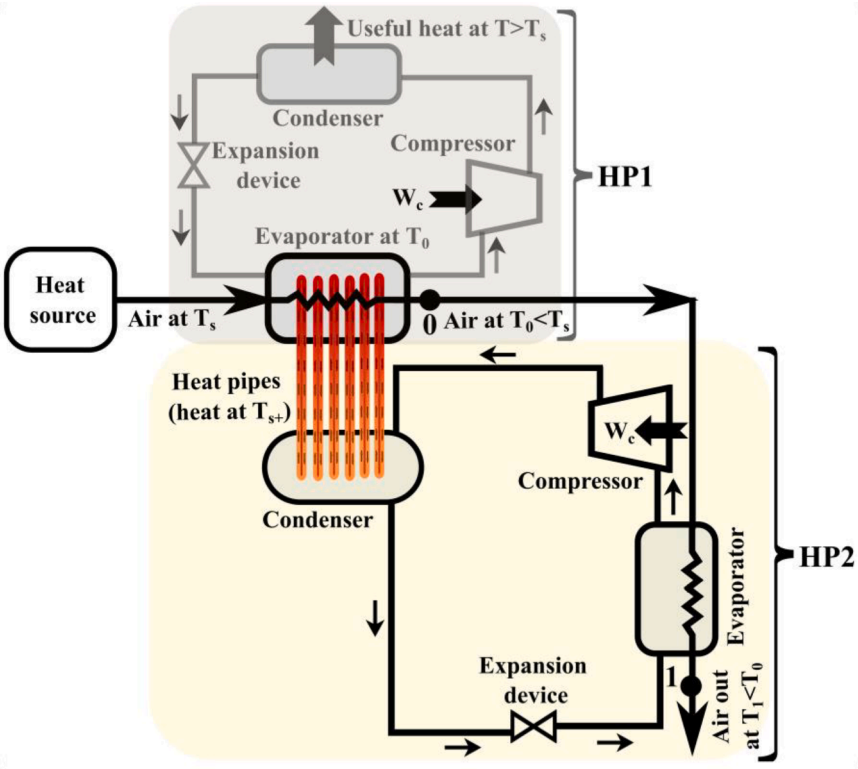	**Pros:** + Well developed technology + Isothermal discharge using heat pipes **Cons:** – Uses high grade energy (electrical/mechanical) – No energy storage option
Configuration 1 (reference): Cascaded conventional HPs.	
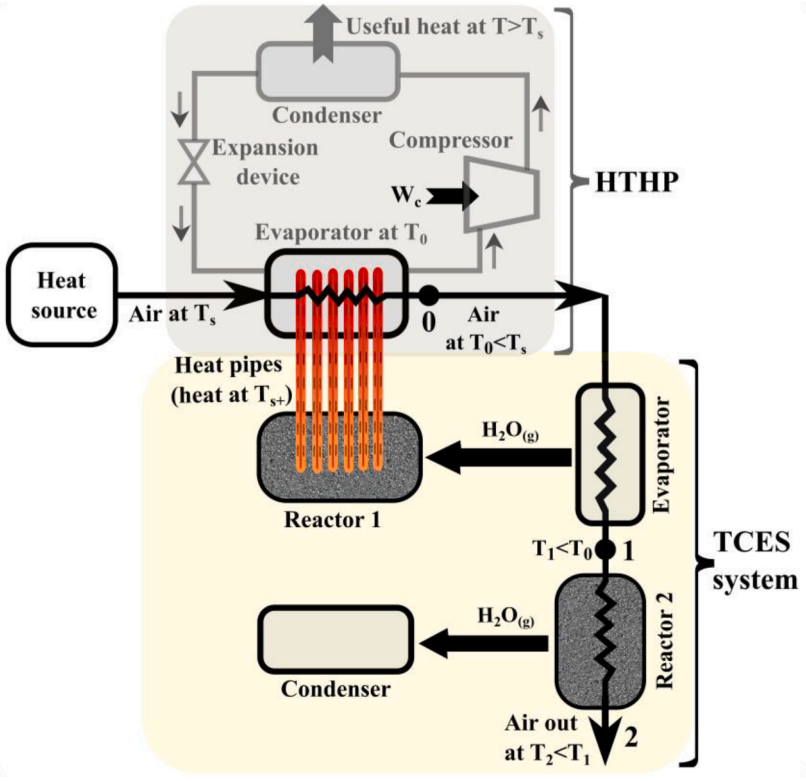	**Pros:** + Thermally driven using waste heat below T_0 + Energy storage option + Closed water vapour system + Isothermal discharge using heat pipes **Cons:** – Vacuum operation of condenser – Requires a well-designed condenser and maintenance due to pressure difference
Configuration 2: Cascaded TCES – HTHP; Indirect charging and indirect discharging.	

(*continued on next page*)

Table 1 (*continued*)

System configuration	Pros and Cons
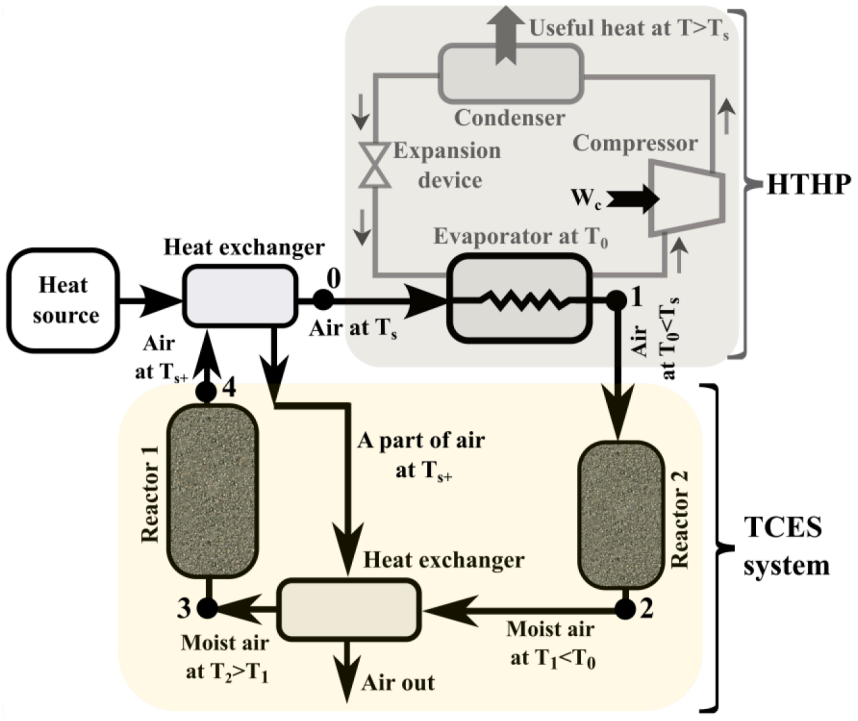	**Pros:** + Thermally driven using waste heat below T_0 + Energy storage option + Pressure-less operation + Direct contact heat transfer with HTF **Cons:** – Sensible heat loss between T_{s+} and T_s during heat delivery – Heat delivery temperature must be significantly higher than the evaporator temperature
Configuration 3: Cascaded TCES – HTHP; Direct charging and direct discharging.	
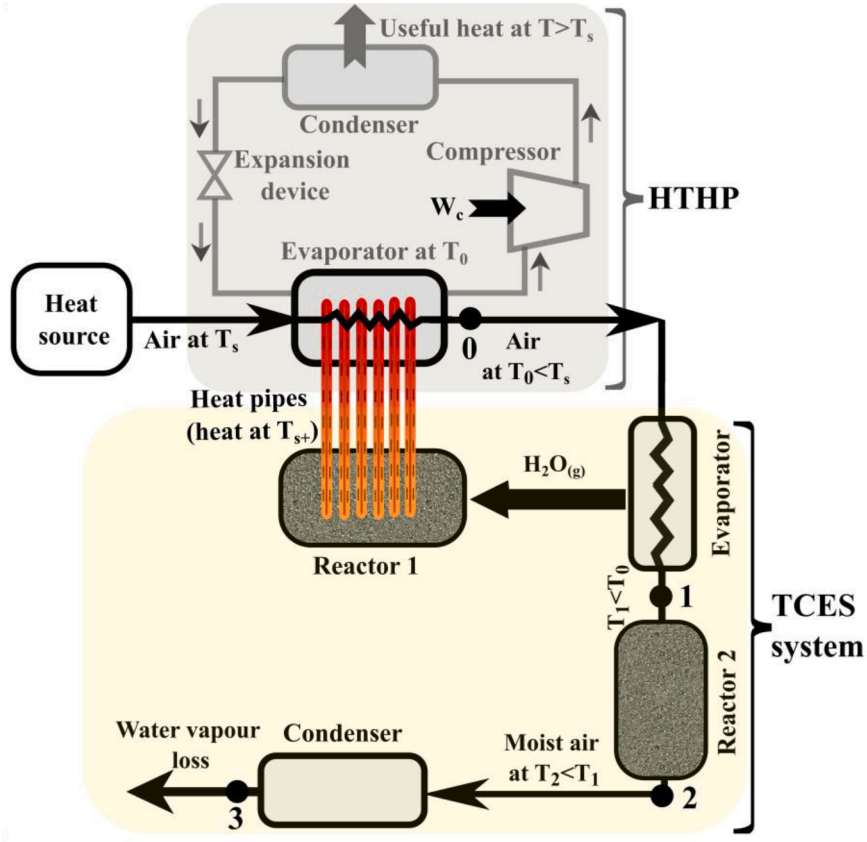	**Pros:** + Thermally driven using waste heat below T_0 + Energy storage option + Pressure-less operation leads to design feasibility + Isothermal discharge using heat pipes **Cons:** – Some quantity of water vapour loss
Configuration 4: Cascaded TCES – HTHP; Direct charging and indirect discharging.	

Here, heat below HP1's evaporator temperature is elevated utilizing HP2, thereafter supplied back to HP1 as a heat source. Notably, conventional cascaded HPs necessitate significant high-grade energy input (electrical/mechanical work) for their operation. While conventional HTHP systems generally employ an HTF system to transfer heat from the low temperature HP's condenser to the HTHP's evaporator [29,30], this study incorporates heat pipes for better comparison with other configurations.

The primary advantage of a TCES system lies in its feasibility of being thermally driven i.e., the utilization of low-grade energy at a temperature markedly lower than the HTHP's evaporator temperature (T_0). Heat at any temperature below that of the evaporator of HTHP can be harnessed to utilize it for TCES until it is above the temperature of the reactor that is aimed at charging. Configurations 2, 3 and 4 are designed to utilize the advantage of the principle of TCES. In Configurations 2, 3, and 4, Reactor 1 and Reactor 2 are intended to be switched after each half-cycle, i.e., Reactor 1 and Reactor 2 are used for charging and discharging in one half-cycle, respectively, and vice versa in the next half-cycle. Therefore, these systems are designed to function in a quasi-continuous mode. It is important to note that all the three proposed novel configurations are supposed to achieve the necessary heat upgrade and temperature boost, but their performance characteristics will differ significantly due to varying heat transfer capabilities.

Configuration 2 introduces an HTHP cascaded with a TCES system, employing indirect charging and discharging mechanisms. Air supplies heat to the evaporator to generate water vapour that is subsequently utilized to discharge heat from Reactor 1 at the required temperature ($T_{s+} > T_s$), and subsequently goes on to charging Reactor 2. As salt hydrates are pressure-dependent temperature systems, the supply of water vapour at an absolute pressure by the evaporator would facilitate higher heat delivery temperatures. For this configuration of the system, meticulous condenser design is imperative to operate under vacuum pressure, requiring diligent maintenance due to susceptibility to gas leakage owing to pressure differentials. Moreover, indirect heat exchange, compounded by the low effective thermal conductivity of salt hydrates, accentuates thermal resistance, thereby limiting system performance.

Configuration 3 depicts a cascaded TCES-HTHP system operating via direct charging and discharging. Here, air traverses a closed loop, entering Reactor 2 at a temperature lower than HTHP's evaporator temperature and exiting relatively cold and humid post-charging. To ensure the air reaches the requisite heat source temperature (T_{s+}), it undergoes preheating before passing through Reactor 1, where it provides water vapor for an exothermic reaction and collects heat. Nevertheless, air must attain a temperature significantly higher than the evaporator temperature of the HTHP, thereby losing sensible heat due to temperature gradients. This configuration poses more operational challenges since the temperature upgrade relies solely on the partial pressure of water vapor in the air.

The fourth configuration comprises a thermally driven cascaded TCES-HTHP system with direct charging and indirect discharging. It is similar to Configuration 2, but with air directly passing through Reactor 2 for charging, followed by passage through a condenser to recover water vapor. Operating pressure-less, as air circulates in an open loop, enables the condenser to function at ambient conditions. Nonetheless, a portion of water vapor loss to the environment is inevitable as complete condensation may not be attainable with the condenser at the ambient temperature.

In addition to these four, there can be another configuration of a cascaded TCES-HTHP system with indirect charging and direct discharging. However, this may not produce satisfactory results since indirect charging causes greater resistance to heat transfer. The temperature of heat in direct discharging would be much lower, as it is governed by the partial pressure of water vapour present in the moist air that is used for discharging. Also, the direct discharge makes it extremely difficult to keep the air dry and at the required exit temperature.

Considering the above qualitative analysis, Configuration 4 emerges as the most viable solution for the targeted application. Supplying pure water vapor at absolute pressure to Reactor 1 ensures elevated reaction temperatures, while heat pipes facilitate effective and nearly isothermal heat transfer. Concurrently, direct passage of dry air through Reactor 2 enables the maximum utilization of the thermal potential of air for charging. Due to direct contact and no requirement of vacuum maintenance, this configuration can be pressure-less which facilitates a simple reactor and system design. Consequently, Configuration 4 is selected for further scrutiny based on the foregoing analysis.

The functionality of Configuration 4 can be elucidated using a van't Hoff plot, as depicted in Fig. 2. Observing Fig. 2 reveals that the HTHP operates at temperatures higher than T_0, while heat below T_0 can be enhanced leveraging a TCES system. Based on Configuration 4 and Fig. 2, air enters the evaporator of TCES system at T_0 and its thermal energy is harnessed in the evaporator until reaching T_1, facilitating the production of water vapour. Subsequently, the generated water vapor is directed to Reactor 1, generating heat at a temperature corresponding to the salt hydrate's equilibrium pressure, which is then transferred to the HTHP's evaporator via heat pipes. Ideally, it is desirable to generate heat in the Reactor 1 at T_{s+}. The air, at the exit of evaporator at T_1, proceeds to Reactor 2 for charging, where its temperature decreases further to T_2. It subsequently passes through a condenser operating at ambient temperature.

Thus, the proposed novel cascaded HP system pertaining to Configuration 4 is based on using thermal energy below T_0 in two ways: First, the thermal energy between T_0 and T_1 is provided for the evaporation of water at ambient pressure to discharge one reactor at T_{s+} (thermally driving the heat pump). Second, the thermal energy below T_1 and above T_2 is used to drive the charging of the other reactor.

It may be noted that the van't Hoff plot for Configuration 2 appears similar to that of Configuration 4; however, the key distinction lies in the heat transfer method. Configuration 2 utilizes indirect heat transfer, while Configuration 4 employs direct heat transfer in Reactor 2 as described earlier. The direct method is expected to cause a greater temperature drop in the air due to the lower thermal resistance between the air and the salt hydrate bed. Therefore, for Configuration 2 to achieve the same temperature drop in the HTF, it would require more thermal energy input and, as a result, take longer when using air as the HTF under the same operating conditions. This necessitates a longer residence time for the HTF, requiring a specialized reactor design. A

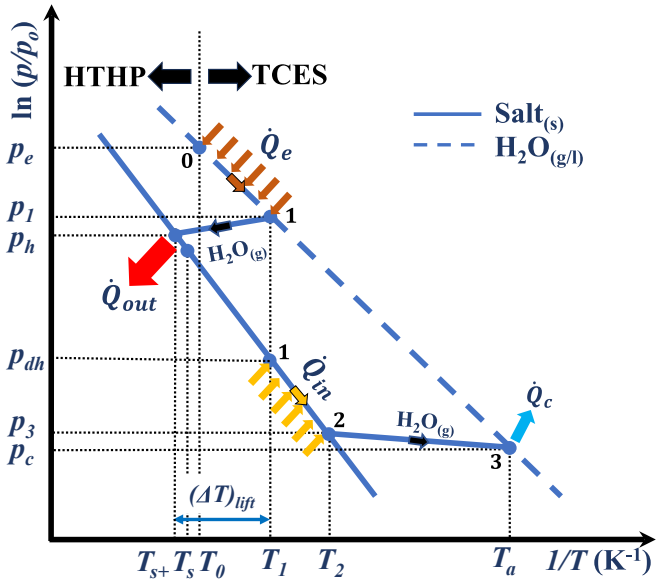

Fig. 2. Van't hoff plot for the operation of the system in configuration 4.

similar rationale applies to Configuration 3.

Upon determining the optimal configuration of the cascaded TCES-HTHP system, its efficacy predominantly hinges upon the characteristics of the salt hydrate material tailored for a specific application within the prescribed operational parameters. Hence, the choice of an appropriate salt hydrate is pivotal in dictating system performance. Subsequent sections discuss the criteria governing the selection of salt hydrates.

Selection and evaluation of suitable salt hydrates for TCES system

Screening of salt hydrates using van't Hoff correlation and compatibility

Choosing an appropriate salt hydrate is crucial for designing a salt hydrate based TCES system, as its performance primarily relies on the characteristics of the selected salt hydrate. The van't Hoff equation (Eq. (2)) can be utilized for the preliminary screening of salts based on the compatibility of equilibrium pressures and temperatures. The present study considers the operating temperatures of the evaporator of the HTHP (T_0) in the range of 105 °C–145 °C. Subsequently, the heat in this temperature range is harnessed to a level of 100 °C (T_1) to generate water vapour at 1 bar pressure in the evaporator of the TCES, which is subsequently used to generate heat in Reactor 1. Further, the waste heat at temperatures below 100 °C is utilized as a driving force for charging the salt hydrate based TCES system. Furthermore, direct charging leads to pressure requirements for water vapour present in the air that need to satisfy the condenser pressures for its recovery. Based on the research conducted by Richter et al. [31], some of the well-studied salt hydrates listed in Table 2 are chosen for screening.

During the charging, the salt hydrate releases water vapour at a pressure corresponding to the temperature of the heat supplied to it. This water vapour can be recovered using a condenser. Therefore, it is desirable to have higher desorption pressures. For instance, the equilibrium pressures of the aforementioned salt hydrates at waste heat temperatures of 80 °C–100 °C are plotted as shown in Fig. 3. It is observed that LiCl, Na_2S, K_2CO_3 and LiBr exhibit relatively higher pressures in the chosen temperature range. $SrBr_2$ is reported to be compatible for open reactor operation, however, its equilibrium pressures are extremely low that it may not fit for direct charging at the intended temperatures.

Though the equilibrium pressures of LiCl and LiBr are relatively high, they have an issue of deliquesce even at very low water vapor pressures [31]. On the other hand, Na_2S is reported to be not suitable for open reactor operations as it degrades after 4 cycles [32]. The literature reports that K_2CO_3 is compatible with closed and open reactor operations due to its chemical stability when directly exposed to air [32]. Also, K_2CO_3 seems advantageous as it provides relatively higher heat delivery temperatures at the same pressures and amounts of water vapor absorption that suit the intended operating temperatures. Additionally, it

Table 2
Salt hydrates selected for initial screening [31].

Salt hydrate	ΔH_r^o (J/mol)	ΔS_r^o (J/mol.K)
$CaCl_2$	73,360	136.53
$SrBr_2$	71,980	143.93
K_2CO_3	64,000	145.82
$SrCl_2$	66,080	131.68
$CaSO_4$	65,880	137.03
$MnBr_2$	78,280	120.00
$ZnSO_4$	82,650	160.83
LiCl	62,150	145.32
LiBr	69,550	153.50
$MgSO_4$	75,380	154.03
$MgCl_2$	71,270	146.73
Na_2S	74,500	177.00
$MnCl_2$	66,790	132.97

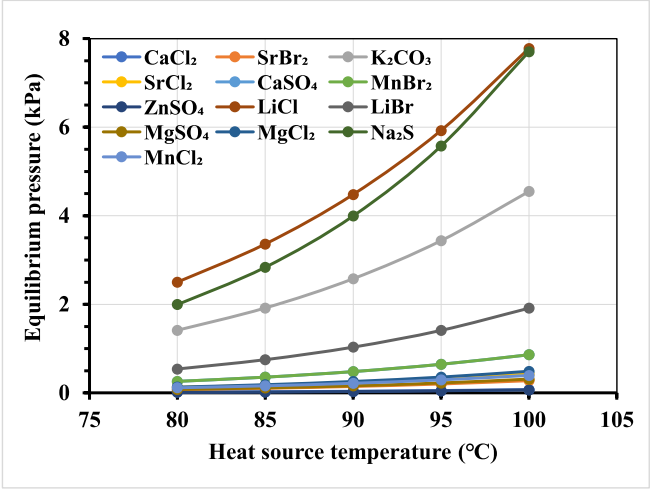

Fig. 3. Van't hoff plots for the selected salt hydrates.

exhibits higher equilibrium pressures at the specified temperatures, which is beneficial for open reactor operations during charging. Moreover, K_2CO_3 is cost-effective, abundantly available, and chemically stable [33]. Recent studies have shown that K_2CO_3 salt hydrate exhibits high specific heating power, large energy storage densities, and significant cyclic stability, making it well-suited for several thermal applications [34,35]. Consequently, K_2CO_3 has been selected in the present study for the subsequent thermodynamic analysis of the performance of material as well as the dual-reactor TCES system integrated with HTHP, as illustrated in Configuration 4 (refer to Table 1).

It is also crucial to understand the maximum possible heat collection by the TCES material during charging as a function of its water vapor content, for determining waste heat utilization capacity with the selected system configuration. Also, it is essential to determine the maximum achievable heat delivery temperatures during TCES system discharge to assess its feasibility for integration with an HTHP. To achieve this, a thermodynamic analysis is conducted in the subsequent section examining air outlet temperatures at various humidities.

Thermodynamic analysis of the selected salt hydrate performance

For the efficient design of an open reactor salt hydrate TCES system, it is essential to comprehend the relationship between air inlet and outlet temperatures as a function of water vapor content. This provides basic insights and lays a foundation for the thermal design of the system. In the following section, first, a correlation to approximate the temperature of air at the outlet of the open reactor during charging is developed using mass and energy balances. Then, a simpler evaluation for the discharging is given.

Determination of charging temperature in open reactor concept

A simple schematic of the charging of an open reactor (referring to Reactor 2 in Configuration 4) is depicted in Fig. 4. In this process, hot air in a dry or low humid state is supplied to the saturated salt hydrate bed. It transfers heat to the salt hydrate bed and collects desorbed water vapour from it, thus exiting the reactor in a relatively cold and humid state. For the sake of simplification of the analysis, a thermal equilibrium is assumed between the salt hydrate bed and water vapour. A steady-state operation is considered and the salt hydrate bed is treated as a lumped system exchanging heat with the HTF. The sensible heat transfer to and from the salt hydrate bed during charging and discharging processes to reach the reaction temperature is neglected. This assumption may be legitimate because, during the charging process, the sensible heat supplied to the reactor can be recovered post-charging by supplying HTF at ambient temperature. Consequently, the reaction heat

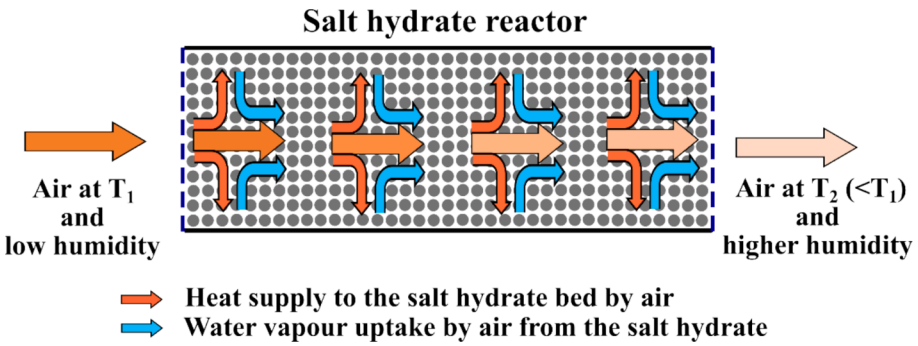

Fig. 4. Schematic of charging a salt hydrate reactor with direct heating.

becomes the most critical factor in these systems. This logic applies equally to the discharging process. Also, it may be noticed that the sensible heat supplied to and recovered from the salt hydrate bed is not included in the energy and efficiency calculations.

Mass balance:

The air stream is composed of both dry air and water vapor. Therefore, the mass balance equations account for the conservation of both dry air and water vapor.

$$\text{Dry air} = \dot{m}_{a2} = \dot{m}_a \tag{3}$$

$$\text{Water vapour} \dot{m}_{wv1} + \dot{m}_{wv} = \dot{m}_{wv2} \tag{4}$$

where $\dot{m}_{a1}$ and $\dot{m}_{a2}$ are the mass flow rates (kg/s) of dry air at the inlet and outlet of the reactor, respectively, which remain constant. $\dot{m}_{wv1}$ and $\dot{m}_{wv2}$ denote the water vapour flow rates at the inlet and outlet of the reactor. $\dot{m}_{wv}$ denotes that rate of water vapour released by the salt hydrate bed during charging. Eq. (4) can be written as,

$$\dot{m}_{a1}\omega_1 + \dot{m}_{wv} = \dot{m}_{a2}\omega_2$$

where ω_1 and ω_2 indicate the specific humidity (kg of water vapour per kg of dry air, denoted in this study as kgWV/kgDA) at the inlet and outlet of the reactor, respectively. The rate of water vapour released during the charging can be written as,

$$\dot{m}_{wv} = \dot{m}_a(\omega_2 - \omega_1) \tag{5}$$

Energy balance:

Considering the salt hydrate bed as the control volume (cv), the steady state energy balance equation for air can be written as,

$$\dot{Q}_{cv} = \dot{m}_{a1}h_1 - \dot{m}_{a2}h_2 \tag{6}$$

here h_1 and h_2 are the enthalpies (J/kg) of moist air at the inlet and outlet, respectively. Enthalpy of moist is the total enthalpy of dry air and moist air ($h = h_a + \omega h_{wv}$). Considering dry air as an ideal gas, its enthalpy can be written as,

$$h_a = c_{p,a}T \tag{7}$$

where $c_{p,a}$ (J/kg.K) is the specific heat capacity of dry air at a constant pressure. The enthalpy of water vapour in the moist air can be written as [36],

$$h_{wv} \cong 2500.9 + 1.82T, \quad (T \text{ in } ^\circ\text{C}) \tag{8}$$

Heat exchange in the control volume is,

$$\dot{Q}_{cv} = \dot{Q}_r + \dot{Q}_{wv} \tag{9}$$

During the charging, the inlet hot air provides the heat of reaction ($\dot{Q}_r$) to the salt hydrate bed and a part of heat is carried away by the water vapour released ($\dot{Q}_{wv}$). Also, the rate of water vapour release indicates the reacted fraction of the salt hydrate bed.

$$\dot{Q}_r = \dot{m}_{wv}\Delta H_r^o$$

Sensible heat transfer to water vapour,

$$\dot{Q}_{wv} = \dot{m}_{wv}c_{p,wv}(T_1 - T_i)$$

Therefore, Eq. (9) can be written as,

$$\dot{Q}_{cv} = \dot{m}_{wv}\Delta H_r^o + \dot{m}_w c_{p,wv}(T_1 - T_i)$$

Thus, Eq. (6) becomes,

$$\dot{m}_{a2}h_2 = \dot{m}_{a1}h_1 - \dot{m}_{wv}\Delta H_r^o - \dot{m}_{wv}c_{p,wv}(T_1 - T_i)$$

$$\dot{m}_{a2}h_2 = \dot{m}_{a1}h_1 - \dot{m}_a(\omega_2 - \omega_1)\Delta H_r^o - \dot{m}_a(\omega_2 - \omega_1)c_{p,wv}(T_1 - T_i)$$

$$h_2 = h_1 - (\omega_2 - \omega_1)\Delta H_r^o - (\omega_2 - \omega_1)c_{p,wv}(T_1 - T_i)$$

$$c_{p,a}T_2 + (2501 + c_{p,wv}T_2)\omega_2 = c_{p,a}T_1 + (2501 + c_{p,wv}T_1)\omega_1 - (\omega_2 - \omega_1)\Delta H_r^o - (\omega_2 - \omega_1)c_{p,wv}(T_1 - T_i)$$

$$T_2 = \frac{c_{p,a}T_1 + (2501 + c_{p,wv}T_1)\omega_1 - (\omega_2 - \omega_1)(\Delta H_r^o + c_{p,wv}T_1 - c_{p,wv}T_i) - 2501\omega_2}{c_{p,a} + c_{p,wv}\omega_2} \tag{10}$$

In the above equation, $c_{p,wv}$ (J/kg.K) is the specific heat capacity of water vapour. ω, the specific humidity of air is estimated as,

$$\omega = \frac{0.622 \times \phi \times p_g}{p - \phi \times p_g} \tag{11}$$

where ϕ and p_g (kPa) are the air relative humidity and saturation pressure of water, respectively.

Limiting conditions for charging:

- To prevent condensation within the reactor, vapour pressure of air passing through the salt hydrate bed must be less than its saturation pressure corresponding to its outlet temperature, i.e., the relative humidity (Φ) of air in the reactor should be less than 100 %.

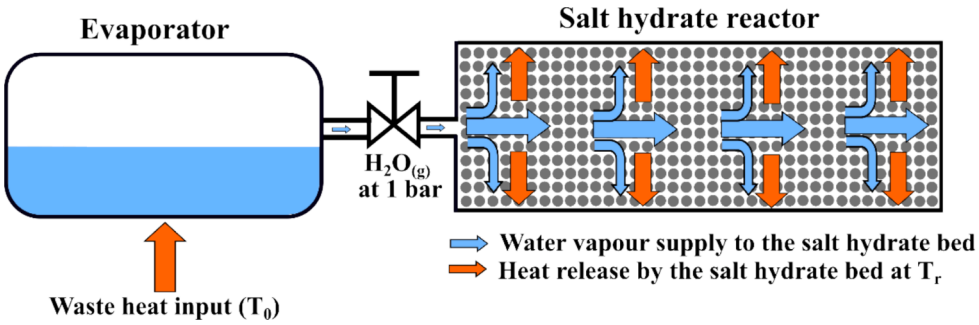

Fig. 5. Schematic of discharging a salt hydrate reactor with indirect heat recovery.

The saturation pressure of air is estimated using Tetens equation [37];

$$p_g = 0.61078 \times \exp\left(\frac{17.27 \times T}{T + 237.3}\right), \quad (T\,in\,°C \text{ and } pg\,in\,kPa.) \tag{12}$$

Discharging temperature

A simple schematic of the heat discharge with a closed reactor coupled with an evaporator (referring to Reactor 1 in Configuration 4) is shown in Fig. 5. In this operation, water vapour is generated in an evaporator using the waste heat of the HTHP and fed to Reactor 1 for hydration reaction.

In this study, water vapour is aimed to be generated and supplied to Reactor 1 at the atmospheric pressure (1 bar) to enable the utilization of cost-efficient pressure-less components. It is driven by the waste heat of the HTHP in the temperature range of 105 °C–145 °C, thus, the evaporator is operated at 100 °C (T_1). The hydration reaction (discharge) temperature (T_r *or* T_{s+}) of salt hydrates is calculated corresponding to the 1 bar water vapour pressure using the van't Hoff equation mentioned in Eq. (2). For the efficient feeding of discharged heat to the HTHP, heat pipes are incorporated in Reactor 1 as shown in Configuration 4. Please notice that the heat pipes are not shown in Fig. 5.

Limiting conditions for discharging (hydration):

- Heat discharging temperature (T_{s+}) should be higher than the HTHP's evaporator temperature (T_0).

Performance analysis of K_2CO_3

Further investigation following the mathematical equations for direct charging in Reactor 2 and indirect discharging in Reactor 1 is performed on K_2CO_3. This analysis helps in understanding the required reacted fraction of the salt hydrate to achieve the intended energy output and assists in designing the system effectively.

Charging

To evaluate the proposed concept of direct charging, the outlet temperatures of air during the direct charging process are estimated across various humidity levels. According to Configuration 4 of the proposed cascaded heat pump, air enters Reactor 2 in a dry state (Φ_1 = 0andω_1 = 0kgWV/kgDA) at 100 °C (T_1) for charging. The outlet temperature of the air (T_2) is then estimated using Eq. (10) at relative humidity levels ranging from 0 (0 %) to 1 (100 %). It should be noted that Eq. (10) is an implicit function, as the outlet specific humidity of the air (ω_2) is also a function of T_2. For different relative humidity levels of the outlet air (Φ_2), specific humidity levels (ω_2) are determined using Eq. (12). The final expression for ω_2 as a function of T_2 can be formulated as,

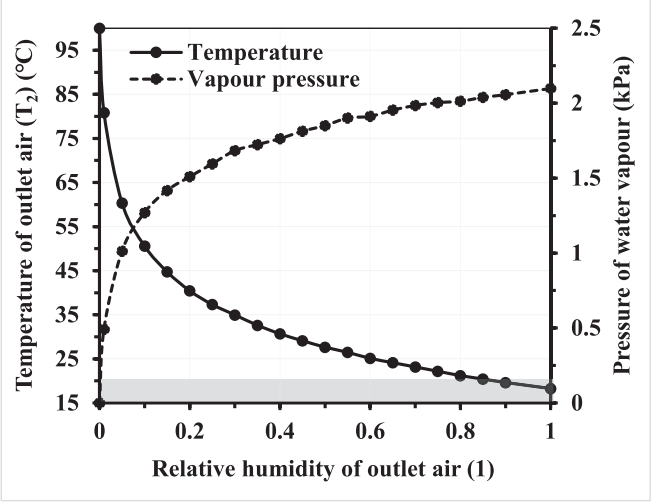

Fig. 6. Variation in the outlet temperature (T_2) of air and vapour pressure with change in the relative humidity during charging at T_1 = 100 °C.

$$\omega_2 = \frac{0.622 \times \Phi_2 \times 0.61078 \times exp\left(\frac{17.27T_2}{T_2+237.3}\right)}{p - \Phi_2 \times 0.61078 \times exp\left(\frac{17.27T_2}{T_2+237.3}\right)} \tag{13}$$

To solve for T_2 at various outlet relative humidity values of air, Eq. (10) is modified by substituting ω_2 with Eq. (13) and the root of the equation is estimated using the bisection method. This calculation is programmed in C++. Variations in the temperature and the water vapour pressure of outlet air as a function of relative humidity are depicted in Fig. 6.

During the charging of an open reactor with hot air, the relative humidity at the reactor exit indicates the extent of the utilization of air for charging. A higher exit relative humidity signifies greater water vapor absorption from the salt hydrate bed, indicating that the air has supplied more heat for charging, resulting in a significant drop in its temperature. This effect is shown in Fig. 6. It is noticed that the air temperature decreases substantially with increasing outlet humidity as it supplies water vapour to K_2CO_3 bed. During the direct charging, 10 % relative humidity of output air causes a 19.1 °C drop in air temperature, whereas 40 % results in a 60 °C drop. This suggests that careful design of a salt-hydrate reactor and optimization of operating parameters are required to ensure a defined outlet humidity and the optimum output temperatures. The grey area in Fig. 6 represents infeasible operating conditions where the air temperature drops below the initial temperature of the salt hydrate bed (20 °C). The vapor pressure of the outlet air determines the necessary conditions for the condenser to extract water from the air. Specifically, the condenser's saturation pressure must be

lower than the vapor pressure of water in the outlet air to facilitate condensation. As Fig. 6 depicts, as the outlet air temperature decreases, the vapor pressure increases significantly, indicating that more heat is being supplied to the salt hydrate bed, which enhances the dehydration reaction.

Discharging

The discharge temperature (T_{s+}) of K_2CO_3 corresponding to 1 bar water vapour pressure in a direct reactor concept can be estimated using Eq. (2) to 165.75 °C. The discharge temperature of the salt hydrate considered for the study is significantly higher than the specified evaporator temperatures (T_0) of the HTHP, i.e., 105 °C–145 °C. The use of heat pipes to deliver the upgraded heat back to the HTHP, as presented in the proposed system configuration, ensures effective heat transfer.

The above analysis can also be performed on other salt hydrates that satisfy the basic requirements of open reactor operations and the temperature requirements of an intended application, as discussed in Section 4. In the present study, this analysis is performed only on K_2CO_3, as it is found to be the most suitable material among the chosen salt hydrates.

Thermodynamic analysis of the TCES system of configuration 4

In this section, a thermodynamic analysis is performed on Configuration 4 shown in Section 3 to evaluate the feasibility of cascaded TCES-HTHP. The analysis focuses on the TCES with K_2CO_3 bed in both reactors and the temperature of air at the inlet of the evaporator (T_0) of TCES is varied from 105 °C to 145 °C. The evaporator of TCES is considered to operate at the atmospheric pressure and thus at 100 °C (T_1), and the air temperature at the exit of the evaporator is assumed to be equivalent to the evaporator temperature. As a result, the HTF experiences a temperature change of 5 K–45 K as it passes through the evaporator, depending on the waste heat temperature. Consequently, the evaporator generates an equivalent amount of water vapour corresponding to the amount of thermal energy it receives from the HTF. It is to be noticed that the evaporator supplies water vapour at a minimum pressure of 101.325 kPa because it is operated at 100 °C irrespective of the temperature of waste heat (105 °C to 145 °C). Therefore, the reaction heat temperature in Reactor 1 would always be ideally the same as it is a function of water vapour pressure. However, the total amount of thermal energy generated in Reactor 1 varies with the amount of water vapour supplied to it, which is a function of the heat supplied to the evaporator. The condenser is intended to operate at a typical ambient temperature of 20 °C (T_a).

Using the stoichiometric equation of K_2CO_3/H_2O reaction, its energy storage density is calculated.

$$K_2CO_3(s) + 1.5H_2O(g) \leftrightarrow K_2CO_3 \bullet 1.5H_2O(s) + \Delta H_r^o \Delta H_r^o = 64\text{kJ/mol} \tag{14}$$

Based on the stoichiometric equation, the weight percentage of water vapour in a saturated potassium carbonate hydrate is estimated to be 16.355 %. Therefore, each kg of K_2CO_3 salt hydrate can absorb 163.55 g of water vapour in its saturated state. This implies that when K_2CO_3 reacts with 1 kg of water vapour, it releases 3.575 MJ of heat.

Evaluation of the TCES system performance

The available waste heat from the HTF,

$$\dot{Q}_{HTF} = \dot{m}_a \times c_{p,a} \times (T_0 - T_a) \tag{15}$$

Evaporator of TCES: The air stream at the outlet of the evaporator of the HTHP is first used to generate water vapour in the evaporator of the TCES system. The heat supplied to the evaporator ($\dot{Q}_{in,E}$) and the rate of water vapour evaporation ($\dot{m}_{wv,E}$) are estimated as,

$$\dot{Q}_{in,E} = \dot{m}_{wv,E} \times \Delta H_e + \dot{m}_{wv,E} \times c_{p,w} \times (T_1 - T_a) \tag{16}$$

where ΔH_e (J/kg) is the latent heat of evaporation. The heat transfer due to the change in enthalpy of air across the evaporator is,

$$\dot{Q}_{a,E} = \dot{m}_a \times (h_0 - h_1) = \dot{m}_a \times c_{p,a} \times (T_0 - T_1) \tag{17}$$

Eqs. (16) and (17) are equal because of the energy balance between the air and the evaporator. It may be noticed that, in addition to the latent heat of evaporation, Eq. (16) also considers the sensible heat required for the evaporated water vapour to reach its evaporation temperature from the ambient temperature.

Reactor 1 of TCES: The water vapour generated in the evaporator of TCES system is supplied to Reactor 1. Here, using the rate of supply of water vapour and the enthalpy of reaction of K_2CO_3, the rate of heat generated is estimated. The reaction temperature corresponding to the equilibrium pressure of water vapour is estimated with the help of Eq. (2).

$$\text{Rate of heat generated by Reactor 1, } \dot{Q}_{gen,R1} = \dot{m}_{wv,E} \times \Delta H_r^o \tag{18}$$

Reactor 2 of TCES: Following the evaporator, the air stream passes through Reactor 2, where its thermal energy is harnessed to charge the reactor. The heat transfer due to the change in enthalpy of air across Reactor 2 is estimated as,

$$\dot{Q}_{a,R2} = \dot{m}_a \times \left(h_{in,R2} - h_{out,R2}\right) \tag{19}$$

where h (J/kg) is the enthalpy of moist air which corresponds to the sum of the enthalpies of dry air (h_a) and water vapour (h_g).

The heat supplied to Reactor 2 during charging can be obtained based on the quantity of water vapour released as,

$$\dot{Q}_{in,R2} = \dot{m}_{wv,R2} \times \Delta H_r^o + \dot{m}_{wv,R2} \times c_{p,wv} \times (T_1 - T_2) \tag{20}$$

Obviously, following Configuration 4, one important constraint considered in this study is that the rate of water vapour consumed by Reactor 1 is equal to the rate of water vapour released by Reactor 2. Therefore, using Eqs. (17), (19) and (20), the outlet temperature of air T_2 can be obtained as function of T_1 as,

$$T_2 = \frac{\left(\Delta H_r^o + c_{p,wv} \times T_1\right) \times \left(c_{p,a} \times (T_0 - T_1)\right) - \left(\Delta H_e + c_{p,w} \times (T_1 - T_a)\right) \times \left(c_{p,a} \times T_1 - 2501 \times \omega_2\right)}{c_{p,a} \times c_{p,wv} \times (T_0 - T_1) + \left(\Delta H_e + c_{p,w} \times (T_1 - T_a)\right) \times \left(-c_{p,a} - 1.82 \times \omega_2\right)} \tag{21}$$

It may be noticed that the heat input from the air for the dehydration reaction is substantially higher than the sensible heat carried away by the water vapour. Furthermore, due to the constraint of equivalent water vapour generated by the evaporator and Reactor 2, using Eqs. (16) and (20), it is realized that the ratio of air temperature change across the evaporator and Reactor 2 remains constant at any heat source temperature (T_o).

$$\frac{T_0 - T_1}{T_1 - T_2} = \frac{\Delta H_e + c_{p,w} \times (T_1 - T_a)}{\Delta H_r^o + c_{p,wv} \times (T_1 - T_2)} = Constant \quad (22)$$

The above equation considers that the fraction of water vapour in moist air is negligible compared to the dry air.

Condenser of TCES: The water vapour released during charging of Reactor 2 is condensed using an air-cooled condenser, operated at ambient temperature, and the condensation rate is estimated to assess the loss of water vapour to the environment.

$$\dot{Q}_{out,C} = \dot{m}_a \times \left(h_{in,C} - h_{out,C}\right) = \dot{m}_{wv,C} \times \Delta H_c \quad (23)$$

where ΔH_c (J/kg) is the latent heat of condensation. It should be noted that evaluating heat balance using the condensation rate of water vapour is valid only when the process is isothermal and the vapour pressure of air is higher than its saturation pressure at the condenser temperature. Otherwise, air experiences only sensible cooling which can be quantified using its temperature change across the condenser and its mass flow rate.

Performance indices

In addition to the rate of heat output and loss of water vapour, the following indices are considered to evaluate the performance of the system.

$$\textbf{Efficiency of TCES}, \eta(\%) = \frac{Heat delivery by TCES system}{Heat supplied to TCES system} \times 100 = \frac{\dot{Q}_{gen,R1}}{\dot{Q}_{in,E} + \dot{Q}_{in,R2}} \times 100 \quad (24)$$

$$\textbf{Efficiency of heat upgrading}(\%) = \frac{Heat delivery by TCES system}{Available waste heat from HTHP} \times 100 = \frac{\dot{Q}_{gen,R1}}{\dot{Q}_{HTF}} \times 100 \quad (25)$$

$$\textbf{Overall efficiency}(\%) = \frac{Heat utilized by TCES system}{Available waste heat from HTHP} \times 100 = \frac{\dot{Q}_{in,E} + \dot{Q}_{in,R2}}{\dot{Q}_{HTF}} \times 100 \quad (26)$$

Results and discussion

The results of thermodynamic analysis of the dual-reactor TCES system shown in Configuration 4 are presented and discussed in this section.

Fig. 7 shows the thermal performance of the TCES system. For the generalization of the concept, the rates of heat input and output are presented per kg/s of air $\left(\frac{\dot{Q}_{in/out}[kW_{th}]}{\dot{m}_{HTF}[kg/s]}\right)$. It is noticed that both the heat input and output rise significantly with waste heat temperature (T_0). This fits perfectly for HTHPs that should reach high sink temperatures with high COPs. The rate of heat output by Reactor 1 is determined by its rate of hydration, which is determined by the rate at which it receives water vapour from the evaporator. The water vapour production rate in the evaporator is proportional to the rate of heat it receives from the HTF (air). As the waste heat source temperature (T_0) rises, so does the heat supply to the evaporator due to increased temperature difference. This is because the evaporator is considered to operate at a fixed temperature of 100 °C (T_1). Similarly, the rate of heat supply to the Reactor 2 also increases as the rate of water vapour desorption by Reactor 2 is considered equal to the rate of water vapour absorption by Reactor 1. In absolute numbers, the total heat input to the TCES system is estimated to increase more significantly as compared to heat output, because it is quantified as the total heat supply to both the evaporator and Reactor 2. At a waste heat temperature of 105 °C, the heat supply to the evaporator and Reactor 2 is found to be 5.05 kW and 6.92 kW per kg/s of air, respectively. This is estimated to increase to 45.45 kW and 62.28 kW per kg/s of air at 145℃, respectively. Meanwhile, the heat delivered by Reactor 1 is projected to be 6.92 kW and 62.28 kW per kg/s of air at 105 °C and 145 °C, respectively. The thermal efficiency of the TCES, representing the ratio between the heat supplied and the heat released, remains constant with increase in temperature. This is because, due to the constraint of equal water vapour absorption and desorption by Reactor 1 and Reactor 2, the rate of generation of heat scales at the same rate as the heat input as the supply temperature rises. The efficiency for the considered material K_2CO_3 is observed to be 57.81 %, as depicted in Fig. 7.

The variation in the outlet temperature (T_2) of air post-charging Reactor 2 and its vapour pressure with waste heat temperature (T_o) are plotted as shown in Fig. 8. Across a range of temperatures spanning from 105 °C to 145 °C, waste heat from the air is efficiently utilized to initiate water vapor generation in the evaporator until it attains 100 °C. As mentioned before, the rate of water vapour generation increases with an increase in the heat source temperature due to the increased temperature difference. Increased heat supply to the evaporator leads to greater water vapor provision to Reactor 1, consequently resulting in

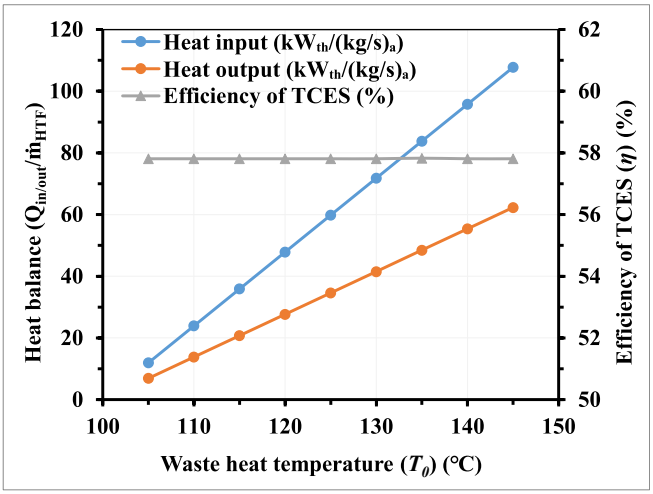

Fig. 7. Thermal performance of the TCES system.

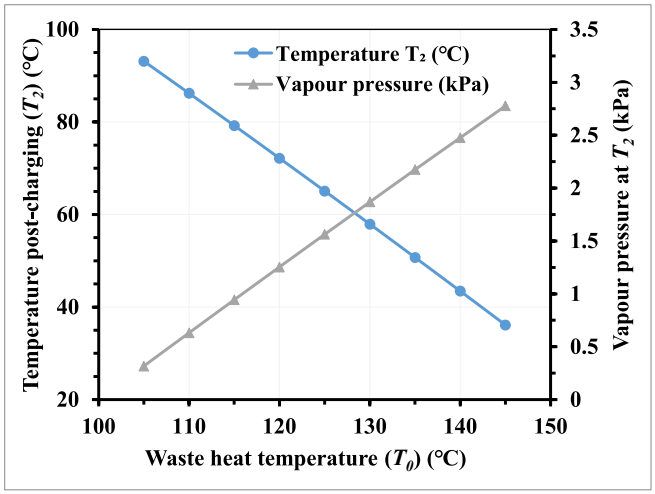

Fig. 8. Temperature of air and its vapour pressure.

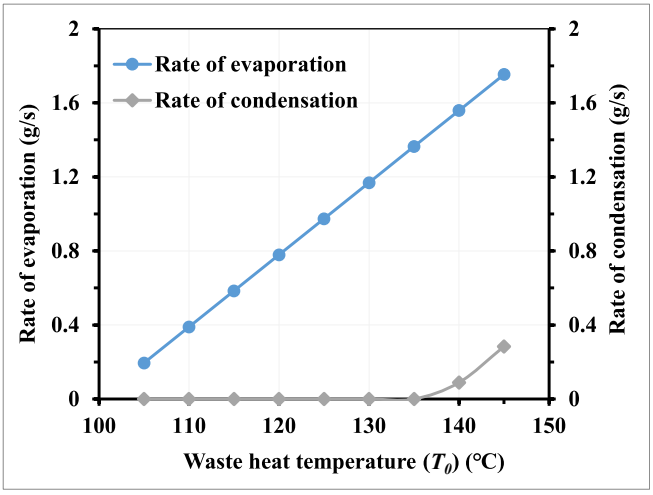

Fig. 9. Recovery of water vapour.

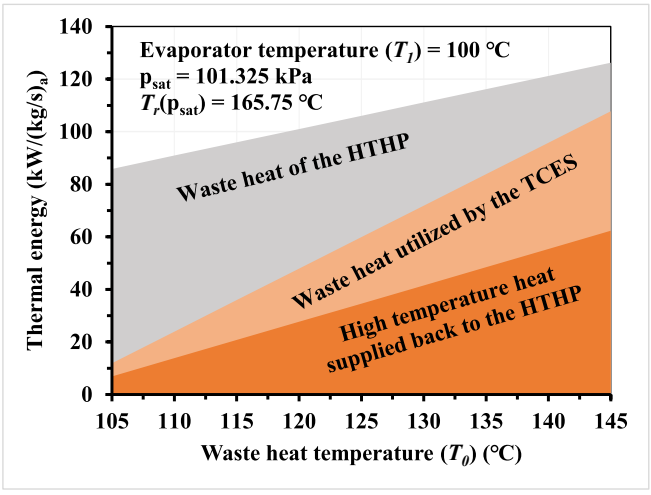

Fig. 10. Overall performance of the cascaded TCES-HTHP system.

higher heat delivery. With Reactor 2 releasing water vapor at an equivalent rate to Reactor 1's intake from the evaporator, the air is expected to provide more heat to Reactor 2 to facilitate increased water vapor desorption at higher temperatures. Consequently, the reduction in air outlet temperature becomes more pronounced at elevated waste heat temperatures, as evidenced in Fig. 8. In other words, the energy in the air mass flow rate is used down to a lower temperature level at higher waste heat temperatures. At 105 °C, due to a small temperature difference of 5 K, water evaporation rate in the evaporator is low (0.195 g/s), leading to a modest demand for water vapour release from Reactor 2. As a result, the air temperature across Reactor 2 decreases by only 6.88 K, indicating that 73.12 K of sensible energy in HTF that could be used is wasted. Conversely, with increased waste heat temperature, evaporation escalates significantly in the evaporator. At 145 °C, water evaporation reaches 1.753 g/s, resulting in a notable 63.88 K drop in air temperature across Reactor 2.

In all the cases examined, the vapor pressure of air at the outlet of Reactor 2 is significantly lower than its saturation pressure, corresponding to its temperature, indicating no chance/issue of condensation within Reactor 2. The lower exit temperatures of air denote a heightened degree of dehydration, resulting in increased water vapor release from K_2CO_3 bed and consequently leading to a substantial increase in the vapor pressure of air, as depicted in Fig. 8. At the outlet temperature (T_2) of 93.12 °C, the vapor pressure is determined to be 0.316 kPa, whereas it reaches 2.778 kPa at 36.12 °C.

Fig. 9 illustrates the rate of water vapor released by Reactor 2 and the fraction of water vapor that could not be recuperated by the condenser operating at ambient temperature. It is to be recalled that the present thermodynamic analysis considers that the rate of water vapor desorbed by Reactor 2 during charging equates to the rate of water vapor absorbed by Reactor 1 from the evaporator, ensuring operational consistency. As previously mentioned, the condenser operates at an ambient temperature of 20 °C with the objective of cooling the air post-charging Reactor 2 to this temperature. As the air temperature decreases within the condenser, its saturation pressure reduces, leading to a reduction in its capacity to retain water vapor. Therefore, if the vapor pressure exceeds the condenser's saturation pressure at the same temperature, condensation initiates until equilibrium is attained with the condenser. As indicated in Table 3, at a waste heat temperature of 105 °C, the air temperature at the condenser inlet is estimated as 93.12 °C. Under this condition, the specific humidity and vapor pressure of air are estimated to be 0.0020 kgWV per kgDA and 0.316 kPa, respectively. Using Eq. (12), the saturation vapor pressure of air and the corresponding specific humidity at 20 °C are computed to be 2.339 kPa and 0.01470 kgWV per kgDA, respectively. It is crucial to note that specific humidity remains constant unless condensation occurs, while relative humidity changes. Condensation occurs when the relative humidity exceeds its maximum value (1) at that specific temperature and pressure. Therefore, even as the air is cooled from 93.12 °C to 20 °C, condensation does not transpire in the condenser due to its relative humidity being lower (0.1353) than its saturated value (1). This scenario is noticed to remain consistent for all other waste heat temperatures except at 140 °C and 145 °C. In these instances, the specific humidity of air (thus, its relative humidity) exceeds its saturated value at 20 °C, leading to the condensation of excess water vapor. The corresponding condensation rate in these two cases is estimated to be 0.089 and 0.284 g/s, respectively. The results indicate that the proposed approach involves the release of water vapour to the ambient.

Fig. 10 depicts the overall performance of the cascaded TCES-HTHP system, including the total available thermal energy of the waste heat from the HTHP, the portion of waste heat utilized by the TCES system, and the portion of heat upgraded and supplied back to the HTHP at a higher temperature than that of the HTHP's evaporator. The portion of heat utilized by the thermochemical heat pump increases with an

Table 3
Humidity and vapour pressure of air at different waste heat temperatures (T_0).

T_0 (°C)	T_2 (°C)	$\dot{m}_{wv,E}$(g/s)	ω_2 at T_2 (kgWV/kgDA)	p_v at T_2 (kPa)	p_g at T_2 (kPa)	Φ_2 at T_2 (1)	Φ_3 at T_c & $p_{g,c}$ (1)	$\dot{m}_{wv,C}$(g/s)
105	93.12	0.195	0.0020	0.316	79.365	0.0040	0.1353	0
110	86.19	0.390	0.0039	0.631	60.847	0.0104	0.2697	0
115	79.21	0.585	0.0058	0.943	46.015	0.0205	0.4033	0
120	72.16	0.779	0.0078	1.254	34.261	0.0366	0.536	0
125	65.07	0.974	0.0097	1.562	25.116	0.0622	0.6680	0
130	57.92	1.169	0.0117	1.869	18.088	0.1033	0.7991	0
135	50.71	1.365	0.0136	2.175	12.778	0.1702	0.9300	0
140	43.44	1.558	0.0156	2.477	8.840	0.2802	>1	0.089
145	36.12	1.753	0.0175	2.778	5.980	0.4645	>1	0.284

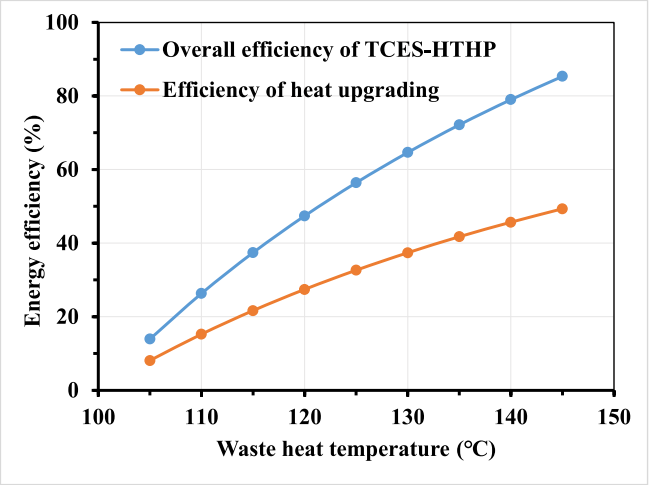

Fig. 11. Overall performance of the cascaded TCES-HTHP system.

increase in the waste heat temperature, and consequently, the heat that is upgraded and reintegrated with the HTHP increases. The evaporator of the TCES produces more water vapour due to the increased temperature difference (T_0-T_1) with an increase in the waste heat temperature (T_0). This is because the evaporator is intended to be operated at 100 °C (T_1) to generate water vapour at 1 bar pressure, resulting in a hydration reaction temperature for K_2CO_3 higher than the operating temperatures of the HTHP's evaporator (T_0 = 105 °C–145 °C). As a result, increasing the amount of water vapour supplied to Reactor 1 generates more heat. At 105 °C, the HTHP produces a waste heat of 85.85 kW, with 11.97 kW utilized and 6.92 kW returned by the TCES per kg/s of air. At 145 °C, these values increase to 126.25, 107.73, and 62.28 kW per kg/s of air, respectively. The difference arises because at 105 °C, sensible heat of air is utilized for a ΔT (T_0-T_2) of 11.88 °C, whereas at 145 °C, it is 108.88 °C. This illustrates the effect of temperature on the efficiency of waste heat utilization by the system.

As previously mentioned, the thermochemical heat pump maintains a consistent efficiency regardless of waste heat temperatures (T_0). This consistency stems from the constant ratio of air temperature change across the evaporator of the TCES and Reactor 2 (Eq. (22)), which is constrained by equal water vapor generation in both components. On the other hand, the overall efficiency of the cascaded TCES-HTHP system rises as waste heat temperature increases. This increase is attributed to the increased potential of sensible heat of the HTF, resulting in more water vapor production in the TCES system's evaporator. Fig. 11 depicts variations in the overall efficiency of the cascaded system with an increase in the waste heat temperature. Increasing the waste heat temperature from 105 °C to 145 °C improves heat upgrading efficiency from 8.06 % to 49.33 %. Similarly, the overall efficiency of the system increases from 13.94 % at 105 °C to 85.33 % at 145 °C.

The above analysis reveals the viability of incorporating a thermally driven salt hydrate heat pump into an HTHP to improve overall efficiency. Using waste heat from the HTHP in the range of 105 °C–145 °C and the evaporator producing water vapour at 1 bar, resulting in a reaction temperature of 165.75 °C for K_2CO_3, demonstrates the possibility of a promising performance. It is to be noticed that K_2CO_3 is employed as a reference material in this study, and the findings of this research are subject to the actual suitability of K_2CO_3. It also presents a framework for the design of a cascaded TCES-HTHP system.

In order to conclude the study for concept 4, two comments on a future reactor and system design can be given for the present dual reactor concept. First of all, in order to realize a continuous thermal upgrade, the two reactors need to be operated in a cycled manner. In this case, the sizing of the reactor is dependent not only on the storage capacity of the salt but also on the rate of hydration / dehydration that can be realized in the system. Reactors 1 and 2 should fully and spontaneously react with all of the water vapour supplied by the evaporator to ensure efficient performance and delivery of desired output. If the rate of hydration reaction of the prescribed salt hydrate is slower than the rate of water vapour supplied by the evaporator, excess water vapour accumulates in the reactor in the absence of a sufficient quantity of salt. Consequently, the reactor must be designed to accommodate a sufficient amount of salt. Thus, the optimum mass of salt required for a specified storage capacity will be a trade-off between the kinetics of the reaction, heat and mass transfer enhancement structures, and cost/weight of the container. Furthermore, the required temperature decline of HTF across each heat exchanger in the system to get the desired thermal output provides sizing parameters for those devices. Second, due to the quasi-continuous nature of the dual reactor concept for the sorption-based system, it is also possible to include a thermal storage effect / thermal buffer into the cascaded heat pump system. This attribute of the system assists in mitigating the instability of primary heat sources in meeting the energy demands. In this case, the sizing of the reactors would also consider additional storage effects that address an increased flexibility in heat / energy supply and demand.

Conclusion and outlook

The study emphasizes the necessity of harvesting and efficiently utilizing the waste heat of high temperature heat pumps. In this regard, it proposes a cascade configuration of a thermally driven dual-reactor salt hydrate system with a high temperature heat pump. The study discusses various concepts and recommends an open reactor design with direct charging and indirect discharging processes.

Next to a preliminary screening of possible salt hydrates, a theoretical framework is developed to determine the outlet temperature of the heat transfer fluid during direct heating, guiding a more detailed selection of potential salt hydrates. Consequently, K_2CO_3 emerges as a favorable candidate for specified operating temperatures, as it is able to be charged with temperatures down to 50 °C while it can be discharged in the range of 120 °C to 165 °C.

A thermodynamic analysis focusing on the final concept, where waste heat is utilized to thermally drive and thermally charge the salt hydrate heat pump, indicates a promising performance with heat delivery of 6.92 kW and 62.28 kW per kg/s of air at 105 °C and 145 °C, respectively. A significant energy efficiency is observed with about 58 % in all the cases studied while delivering heat at a constant reaction temperature of 165 °C by reacting with water vapour at an ambient pressure of 1 bar generated consistently at 100 °C fuelled by the waste heat of the high temperature heat pump. The overall performance of the system increases significantly with waste heat temperature demonstrating a promising performance of the proposed concept.

The study demonstrates the feasibility of a new thermochemical heat pump that is solemnly thermally driven for upgrading and reintegrating waste heat from a high temperature heat pump. This integration enables the high temperature heat pump to upgrade more thermal energy at the same or higher coefficient of performance. In the next step, exergy analysis needs to be carried out, salt hydrates need to be characterized for open reactor operation, and a suitable reactor needs to be designed for an experimental proof of concept.

CRediT authorship contribution statement

K. Malleswararao: Writing – original draft, Visualization, Validation, Supervision, Software, Methodology, Investigation, Formal analysis, Data curation, Conceptualization. **Inga Bürger:** Writing – original draft, Visualization, Supervision, Methodology, Investigation, Formal analysis, Conceptualization. **Aldo Cosquillo Mejia:** Writing – review & editing, Visualization, Supervision, Formal analysis. **Seon Tae Kim:** Writing – review & editing, Supervision. **Marc Linder:** Writing – review & editing, Supervision, Resources, Project administration, Methodology,

Funding acquisition, Conceptualization.

Declaration of competing interest

The authors declare that they have no known competing financial interests or personal relationships that could have appeared to influence the work reported in this paper.

Data availability

No data was used for the research described in the article.

References

[1] Chua KJ, Chou SK, Yang WM. Advances in heat pump systems: a review. Appl Energy 2010;87:3611–24. https://doi.org/10.1016/j.apenergy.2010.06.014.

[2] Sandvall AF, Ahlgren EO, Ekvall T. Low-energy buildings heat supply–modelling of energy systems and carbon emissions impacts. Energy Policy 2017;111:371–82. https://doi.org/10.1016/j.enpol.2017.09.007.

[3] Dong S, Meng X, Hu X, Sun Z, Wang H, Luo Y. Investigation of cascade high temperature heat pump optimal design theory based on experiment supporting multi-objective optimization. Energy Convers Manag 2022;267:115873. https://doi.org/10.1016/j.enconman.2022.115873.

[4] Jarre M, Noussan M, Simonetti M. Primary energy consumption of heat pumps in high renewable share electricity mixes. Energy Convers Manag 2018;171:1339–51. https://doi.org/10.1016/j.enconman.2018.06.067.

[5] Lee D. Experimental study on the heat pump system using R134a refrigerant for zero-emission vehicles. Int J Automot Technol 2015;16:923–8. https://doi.org/10.1007/s12239-015-0094-2.

[6] Gaur AS, Fitiwi DZ, Curtis J. Heat pumps and our low-carbon future: a comprehensive review. Energy Res Soc Sci 2021;71:101764. https://doi.org/10.1016/j.erss.2020.101764.

[7] Fukuda S, Kondou C, Takata N, Koyama S. Low GWP refrigerants R1234ze(E) and R1234ze(Z) for high temperature heat pumps. Int J Refrig 2014;40:161–73. https://doi.org/10.1016/j.ijrefrig.2013.10.014.

[8] Kim J, Park S-R, Baik Y-J, Chang K-C, Ra H-S, Kim M, et al. Experimental study of operating characteristics of compression/absorption high-temperature hybrid heat pump using waste heat. Renew Energy 2013;54:13–9. https://doi.org/10.1016/j.renene.2012.09.032.

[9] Mateu-Royo C, Sawalha S, Mota-Babiloni A, Navarro-Esbrí J. High temperature heat pump integration into district heating network. Energy Convers Manag 2020;210:112719. https://doi.org/10.1016/j.enconman.2020.112719.

[10] Arpagaus C, Bless F, Uhlmann M, Schiffmann J, Bertsch SS. High temperature heat pumps: market overview, state of the art, research status, refrigerants, and application potentials. Energy 2018;152:985–1010. https://doi.org/10.1016/j.energy.2018.03.166.

[11] Wu D, Jiang JT, Hu B, Wang RZ. Experimental investigation on the performance of a very high temperature heat pump with water refrigerant. Energy 2020;190:116427. https://doi.org/10.1016/j.energy.2019.116427.

[12] Kosmadakis G, Arpagaus C, Neofytou P, Bertsch S. Techno-economic analysis of high-temperature heat pumps with low-global warming potential refrigerants for upgrading waste heat up to 150 ℃,. Energy Convers Manag 2020;226:113488. https://doi.org/10.1016/j.enconman.2020.113488.

[13] Zhao A, Pecnik R, Peeters JWR. Thermodynamic analysis and heat exchanger calculations of transcritical high-temperature heat pumps. Energy Convers Manag 2024;303:118172. https://doi.org/10.1016/j.enconman.2024.118172.

[14] Marina A, Spoelstra S, Zondag H, Wemmers A. An estimation of the European industrial heat pump market potential. Renew Sustain Energy Rev 2021;139:110545. https://doi.org/10.1016/j.rser.2020.110545.

[15] Liu C, Han W, Xue X. Experimental investigation of a high-temperature heat pump for industrial steam production. Appl Energy 2022;312:118719. https://doi.org/10.1016/j.apenergy.2022.118719.

[16] Liu C, Jiang Y, Han W, Kang Q. A high-temperature hybrid absorption-compression heat pump for waste heat recovery. Energy Convers Manag 2018;172:391–401. https://doi.org/10.1016/j.enconman.2018.07.027.

[17] Mateu-Royo C, Joaquín NE, Adrián MB, Marta AA, Molés F. Theoretical evaluation of different high-temperature heat pump configurations for low-grade waste heat recovery. Int J Refrig 2018;90:229–37. https://doi.org/10.1016/j.ijrefrig.2018.04.017.

[18] Mateu-Royo C, Arpagaus C, Mota-Babiloni A, Navarro-Esbrí J, Bertsch SS. Advanced high temperature heat pump configurations using low GWP refrigerants for industrial waste heat recovery: a comprehensive study. Energy Convers Manag 2021;229:113752. https://doi.org/10.1016/j.enconman.2020.113752.

[19] Richter M, Bouché M, Linder M. Heat transformation based on $CaCl_2/H_2O$ – Part A: closed operation principle. Appl Therm Eng 2016;102:615–21. https://doi.org/10.1016/j.applthermaleng.2016.03.076.

[20] Bouché M, Richter M, Linder M. Heat transformation based on $CaCl_2/H_2O$ – Part B: open operation principle. Appl Therm Eng 2016;102:641–7. https://doi.org/10.1016/j.applthermaleng.2016.03.102.

[21] Michel B, Dufour N, Börtlein C, Zoude C, Prud'homme E, Gremillard L, Clausse M. First experimental characterization of $CaCl_2$ coated heat exchanger for thermochemical heat transformer applications in industrial waste heat recovery. Appl Therm Eng 2023;227:120400. https://doi.org/10.1016/j.applthermaleng.2023.120400.

[22] Malleswararao K, Dutta P, Srinivasa Murthy S. Applications of metal hydride based thermal systems: a review. Appl Therm Eng 2022;215:118816. https://doi.org/10.1016/j.applthermaleng.2022.118816.

[23] Chen X, Zhang Z, Qi C, Ling X, Peng H. State of the art on the high-temperature thermochemical energy storage systems. Energy Convers Manag 2018;177:792–815. https://doi.org/10.1016/j.enconman.2018.10.011.

[24] Hayatina I, Auckaili A, Farid M. Review on salt hydrate thermochemical heat transformer. Energies 2023;16:4668. https://doi.org/10.3390/en16124668.

[25] Stengler J, Bürger I, Linder M. Thermodynamic and kinetic investigations of the $SrBr_2$ hydration and dehydration reactions for thermochemical energy storage and heat transformation. Appl Energy 2020;277:115432. https://doi.org/10.1016/j.apenergy.2020.115432.

[26] Marias F, Neveu P, Tanguy G, Papillon P. Thermodynamic analysis and experimental study of solid/gas reactor operating in open mode. Energy 2014;66:757–65. https://doi.org/10.1016/j.energy.2014.01.101.

[27] Michel B, Neveu P, Mazet N. Comparison of closed and open thermochemical processes, for long-term thermal energy storage applications. Energy 2014;72:702–16. https://doi.org/10.1016/j.energy.2014.05.097.

[28] Farcot L, Le Pierrès N, Michel B, Fourmigué J-F, Papillon P. Numerical investigations of a continuous thermochemical heat storage reactor. J Energy Storage 2018;20:109–19. https://doi.org/10.1016/j.est.2018.08.020.

[29] Soltani R, Dincer I, Rosen MA. Comparative performance evaluation of cascaded air-source hydronic heat pumps. Energy Convers Manag 2015;89:577–87. https://doi.org/10.1016/j.enconman.2014.10.006.

[30] Jiang J, Hu B, Wang RZ, Deng N, Cao F, Wang CC. A review and perspective on industry high-temperature heat pumps. Renew Sustain Energy Rev 2022;161:112106. https://doi.org/10.1016/j.rser.2022.112106.

[31] Richter M, Habermann E-M, Siebecke E, Linder M. A systematic screening of salt hydrates as materials for a thermochemical heat transformer. Thermochim Acta 2018;659:136–50. https://doi.org/10.1016/j.tca.2017.06.011.

[32] Sögütoglu LC, Donkers PAJ, Fischer HR, Huinink HP, Adan OCG. In-depth investigation of thermochemical performance in a heat battery: cyclic analysis of K_2CO_3, $MgCl_2$ and Na_2S. Appl Energy 2018;205:159–73. https://doi.org/10.1016/j.apenergy.2018.01.083.

[33] Gaeini M, Shaik SA, Rindt C. Characterization of potassium carbonate salt hydrate for thermochemical energy storage in buildings. Energy Build 2019;196:178–93. https://doi.org/10.1016/j.enbuild.2019.05.029.

[34] Houben J, Sögütoglu L, Donkers P, Huinink H, Adan O. K_2CO_3 in closed heat storage systems. Renew Energy 2020;166:35–44. https://doi.org/10.1016/j.renene.2020.11.119.

[35] Mazur N, Blijlevens MAR, Ruliaman R, Fischer H, Donkers P, Meekes H, et al. Revisiting salt hydrate selection for domestic heat storage applications. Renew Energy 2023;218:119331. https://doi.org/10.1016/j.renene.2023.119331.

[36] Cengel YA, Boles MA. Thermodynamics: an engineering approach. sixth ed. McGraw-Hill; 2007.

[37] Monteith JL, Unsworth MH. In: Principles of environmental physics: plants, animals, and the atmosphere. Oxford, UK: Academic Press; 2013. p. 11–3.